Immunohistochemical Localization of Choline Acetyltransferase During Development and in *Cha^{ts}* Mutants of *Drosophila melanogaster*

Michael G. Gorczyca and Jeffrey C. Hall

Department of Biology, Brandeis University, Waltham, Massachusetts 02254

The distribution of choline acetyltransferase (CAT) in the nervous system of Drosophila melanogaster was determined by indirect immunohistochemical procedures using a monoclonal antibody specific to the enzyme. Immunoreactivity was first detected in the nervous system of 16 hr embryos, and increased considerably by the end of embryogenesis. Neuropil was preferentially stained, though cell bodies could also be observed. Staining was prominent in the CNS of all 3 larval instars but decreased substantially during the mid-pupal stage. Prior to eclosion, the level of immunoreactivity increased and the adult staining pattern became discernible. In the adult brain, staining was extensive, with numerous structures, such as the optic lobes and mushroom bodies, staining strongly. The adult thoracic ganglia were also moderately immunoreactive. These results imply a wide distribution of cholinergic neurons in the CNS of Drosophila. Immunoreactivity was also determined for 2 temperature-sensitive CAT mutants, *Cha^{ts1}* and *Cha^{ts2}*. These flies exhibit reduced CAT activity at permissive temperature, 18°C, which eventually falls to undetectable levels after incubation at nonpermissive temperature, 30°C. *Cha^{ts2}* mutants, after incubation at either 18 or 30°C displayed virtually no staining. This result indicated that the immunoreactivity observed in wild-type flies was specifically associated with the enzyme encoded by the Cha gene. The intensity of staining in *Cha^{ts1}* mutants incubated at 18°C appeared greater than in control flies, even though CAT enzyme activity in *Cha^{ts1}* is lower. This suggests that the enzyme molecule itself is structurally altered in *Cha^{ts1}* mutants. After incubation at 30°C, staining in *Cha^{ts1}* flies decreased but did not disappear.

Acetylcholine (ACh) has long been considered to be a major neurotransmitter in the nervous system of insects (Florey, 1963; Gerschenfeld, 1973; Klemm, 1976). In particular, sensory fibers appear to be cholinergic, a conclusion borne out by studies on cercal afferents of *Periplaneta americana* and antennal fibers of *Manduca sexta*. High levels of ACh, its synthetic enzyme, choline acetyltransferase (CAT), and its degradative enzyme, AChE, have been identified in the appropriate regions of these insects'

nervous systems (Treherne, 1966; Sanes and Hildebrand, 1976). Also, α-bungarotoxin (α-BTX) binding sites are present on what seem to be second-order neurons that receive cholinergic input (Sanes et al., 1977; Satelle et al., 1980). In the cockroach, iontophoresis of ACh or of cholinergic agonists produced activity in cells postsynaptic to the mechanoreceptor afferents (Callec, 1976), and AChE inhibitors led to increased activity (Satelle et al., 1980). In addition, both nicotine and α-BTX have been shown to block these apparent synaptic responses (Harrow et al., 1982). It should be noted, however, that several studies in vertebrate CNS indicate that the α-BTX binding site is not identical to the ACh receptor site (Clarke et al., 1985; Smith et al., 1985).

In *Drosophila*, most studies concerned with cholinergic neuron distribution have focused on the CNS or the entire nervous system, not specifically on sensory afferents. In this regard, substantial levels of ACh, CAT, and AChE have been determined throughout most of the life cycle (Dewhurst et al., 1970; Dewhurst and Seecof, 1975; Greenspan, 1980; Greenspan et al., 1980; Salvaterra and McCaman, 1985). α-BTX binding activity has been detected in test-tube assays and in sectioned material (Schmidt-Nielson et al., 1977; Dudai, 1980; Rudloff et al., 1980). *In vitro* binding studies have provided evidence for a muscarinic receptor as well (Dudai, 1980). The *Drosophila* CNS has also been examined with AChE histochemical staining and ³H-choline autoradiography. The patterns of staining and radiolabeling are, however, not always congruent. For example, AChE is found throughout the entire nervous system, whereas choline uptake occurs preferentially in the antennal lobes and mechanosensory neuropil, but is not detectable in the optic ganglia (Buchner and Rodrigues, 1984). To resolve some of these ambiguities, and to achieve a more definitive mapping of cholinergic portions of the CNS in *Drosophila*, we have performed an immunohistochemical analysis of CAT distribution. The value of this approach is that the presence of CAT is considered to be the most reliable evidence for ACh when compared to the aforementioned techniques (Eckenstein, 1985). In addition, the indirect immunofluorescent method of staining used in this report gave superior resolution of neuroanatomical details. Monoclonal antibodies (MAbs) against *Drosophila* CAT have been isolated (Crawford et al., 1982), and preliminary reports of their application in monitoring CAT immunoreactivity have appeared (Ikeda et al., 1984; Salvaterra et al., 1985). We now report a detailed analysis of CAT distribution in the normal and *Cha* mutant nervous systems of adults and in developing animals from embryonic through late pupal stages.

The *Cha* mutations define a gene that almost certainly encodes

the CAT enzyme (Greenspan, 1980; Itoh et al., 1986). Certain of these mutants were isolated on the basis of conditional lethality. Mutant adults, when raised at low temperature (18°C) and then transferred to high temperature (30°C) for 4–5 d, will become paralyzed and die (Greenspan, 1980). Lethality is correlated with temperature-sensitive decrements in CAT activity and ACh synthesis (Greenspan, 1980; Salvaterra and McCaman, 1985). Prior to death, the consequences of these biochemical changes include a cessation of various behaviors and evoked neural responses in the visual system (Greenspan, 1980) and thoracic giant fiber pathway (Gorczyca and Hall, 1984, 1985). By comparing CAT immunoreactivity in the 2 temperature-sensitive *Cha* mutants to that of wild-type, we have shown that the intensity of the staining patterns in *Cha^{ts1}* and *Cha^{ts2}* are markedly different from each other and from normal flies. The intense staining of *Cha^{ts1}* mutants has led us to conclude that their CAT molecules are structurally aberrant. The absence of staining in *Cha^{ts2}* served as a unique genetic control for the specificity of the MAb to CAT.

Materials and Methods

Normal and mutant animals. For CAT immunohistochemistry on developing and adult flies, the *yellow* and *white* (*y w*) pigment mutations were used (except as noted below) because they lead to reduced autofluorescence in the cuticle, eye, and lamina (first-order optic ganglion) when using fluorescein isothiocyanate (FITC) conjugated to the secondary antibody. Genotypes used in experiments on mutants were *Cha^+/Cha^+* (wild-type), *Cha^+/Df-Cha*, *Cha^{ts1}/Df-Cha*, and *Cha^{ts2}/Df-Cha* (these 4 genotypes did not include *y w*). The *Df-Cha* chromosome is deleted for the gene coding for CAT (Greenspan, 1980). Homozygous *Cha^{ts}* mutant stocks were not used because of a possibility that gratuitous recessive mutations might be present on the third chromosomes, elsewhere than at the *Cha* locus. Use of the *Df-Cha* chromosome obviates this potential problem by creating heterozygosity for any deleterious factors at loci other than *Cha*. Flies were maintained on standard cornmeal–agar–molasses–yeast medium and were grown at room temperature. The *Cha^{ts}* mutants and their controls were raised at 18°C (permissive temperature) and transferred to 30°C (non-permissive temperature) for various specified lengths of time.

For selection of staged embryos, adult females were allowed to lay eggs for 2 hr periods on agar-filled petri plates, after which eggs were aged, collected, and dechorionated prior to fixation. Specimens for each of the 3 larval instar stages were selected on the basis of anatomical traits specific to each stage (Bodenstein, 1950). Metamorphosing animals were collected at the white pre-pupa stage from the sides of culture vials. Adults were collected directly from culture bottles every 1–2 d. Only female adults, 2–6 d old, were used. No attempt was made to sex embryos, larvae, or pupae.

Fixation. Dechorionated embryos (see Vallés and White, 1986) of selected ages were placed into a scintillation vial containing equal amounts of heptane and buffered fixative, 4% paraformaldehyde in 0.1 M phosphate buffer, pH 7.2 (Mitchison and Sedat, 1983). The vial was agitated on a shaker bath (300 rpm) for 10 min. Embryos were collected over a nylon mesh, rinsed, and transferred to a deep-welled depression slide from which intact embryos were selected for immunohistochemistry. Vitellin membranes were not removed. Intact larvae could also be fixed with this method.

For most experiments, first and second instar larvae were fixed by pinching off part of the posterior cuticle while it was immersed in buffered 4% paraformaldehyde. The larger size of the third instar larvae necessitated removal of the nervous system, which was dissected from the animal and placed in fixative. This procedure produced optimal staining. Pupae were removed from their cases; their brains were dissected out and placed in fixative. The adult CNS was fixed by placing flies in cold paraformaldehyde and dissecting away the proboscis plus ventral anterior air sacs within the head capsule. This manipulation exposed the entire brain. Other parts of the nervous system, such as the thoracic ganglia, were also fixed but presumably not as quickly, since access to paraformaldehyde was through cuticle and internal tissues. As a general rule, staining intensity was positively correlated to the acces-

sibility of the tissue to fixative; i.e., the strongest staining occurred when the nervous system was directly exposed to paraformaldehyde. Fixation of adult, pupal, and larval material was generally performed for 2 hr. Embryos were fixed briefly (as described above) for 10 min. In some cases, flies were fixed after sectioning, but this consistently caused CAT immunoreactivity to be considerably poorer in intensity and resolution compared with results obtained with material fixed prior to sectioning.

Immunohistochemistry. The following protocol was used for material obtained from any given stage of development. Upon removal from fixative, specimens were placed into a drop of mounting medium (O.C.T.) for 10 min, mounted, and rapidly frozen into a block with CO_2. Subsequently, 10 µm sections were cut on a S.L.E.E. cryotome, and ribbons were picked up on subbed slides. Sections were allowed to air-dry for 10 min and were then rinsed in 0.1 M phosphate buffer (PB), pH 7.2, containing 1% Triton-X 100. After rinsing, they were incubated at 4°C with the anti-CAT MAb termed 1C8 (Crawford et al., 1982) at concentrations of 1–5 µg/ml (in PB with 1% Triton). The primary antibody incubation was generally done overnight but would produce satisfactory results after 2–4 hr. After removal from the cold, sections were rinsed twice in PB for 5 min and incubated with a 1:100 dilution of goat anti-mouse IgG conjugated to FITC (Cappel Laboratories) in PB with 1% Triton for 45 min (or were processed for a HRP staining procedure, see below). This was followed by two 5 min washes in PB and one 5 min wash in 4 mM carbonate buffer, pH 9.5. Sections were mounted in a solution of 20 mM carbonate buffer with 80% glycerol and 0.1% *p*-phenylenediamine (PD), an antiquenching agent that mitigates the bleaching of FITC fluorescence (Platt and Michael, 1983) and were viewed with epi-illumination on a Zeiss inverted microscope with a fluorescein filter set. Specimens were photographed with Kodak Technical Pan film, 2415, which was developed with Kodak HC-110, working dilution F.

HRP was also used as a marker for the primary antibody by employing a Vectastain ABC kit (Vector Laboratories, Pk-4002), involving the avidin–biotin–complex (ABC). The standard ABC protocol was modified in the following manner. Before the primary antibody incubation, horse serum was added to a rinse for 30 min. After the primary incubation, sections were rinsed, then incubated with biotinylated secondary antibody for 3 hr at 29°C. After two 5 min washes in PB, sections were introduced into a solution of 0.6% H_2O_2 in 100% methanol for 5 min to remove endogenous peroxidase activity; this was followed by two 5 min rinses in PB and then by incubation in a biotin–avidin–HRP complex for 3 hr at 29°C. After rinsing in PB, the slides were immersed for 5–10 min into a 0.1 M Tris buffer solution containing 0.05% 3,3'-diaminobenzidine tetrahydrochloride, 0.04% $NiCl_2$, and 0.01% H_2O_2. After rinsing, slides were passed through an ethanol dehydration series and mounted in Permount.

Use of the FITC-protocol was much faster than the HRP-protocol and resulted in far superior resolution. Consequently, it was used in the analysis of CAT distribution in wild-type animals. However, FITC fluorescence decays during photographic exposures; hence, the stable HRP reaction product was a more suitable stain for comparing the levels of immunoreactivity in different genotypes. The intensity of immunoreactivity was compared at various stages of pupal development and also among the *Cha* mutants. To minimize variability in staining intensity that might arise from procedural inconsistencies, specimens to be compared were mounted on the same block and thus were treated identically throughout the entire immunohistochemical procedure. Usually, 4 fly heads, representing 2 each of 2 genotypes or 1 each of 4 genotypes, were processed on the same specimen block together. In addition, several *Cha* mutant flies and wild-type flies were processed only 1 to a block but were concomitantly put through an identical protocol to assess the variability of staining intensity among different blocks processed simultaneously. The results, when comparing the immunoreactivity of the different genotypes, were the same, regardless of which method was used.

Results

Embryos

Anti-CAT staining of specific structures was first observed in 16- to 18-hr-old embryos (from egg-laying). Early to mid-embryos (*n* = 20), 8–16 hr old, showed no signs of immunoreactivity even when incubated with high concentrations (5 µg/ml) of primary antibody for 36 hr. Of twelve 16- to 18-hr-old an-
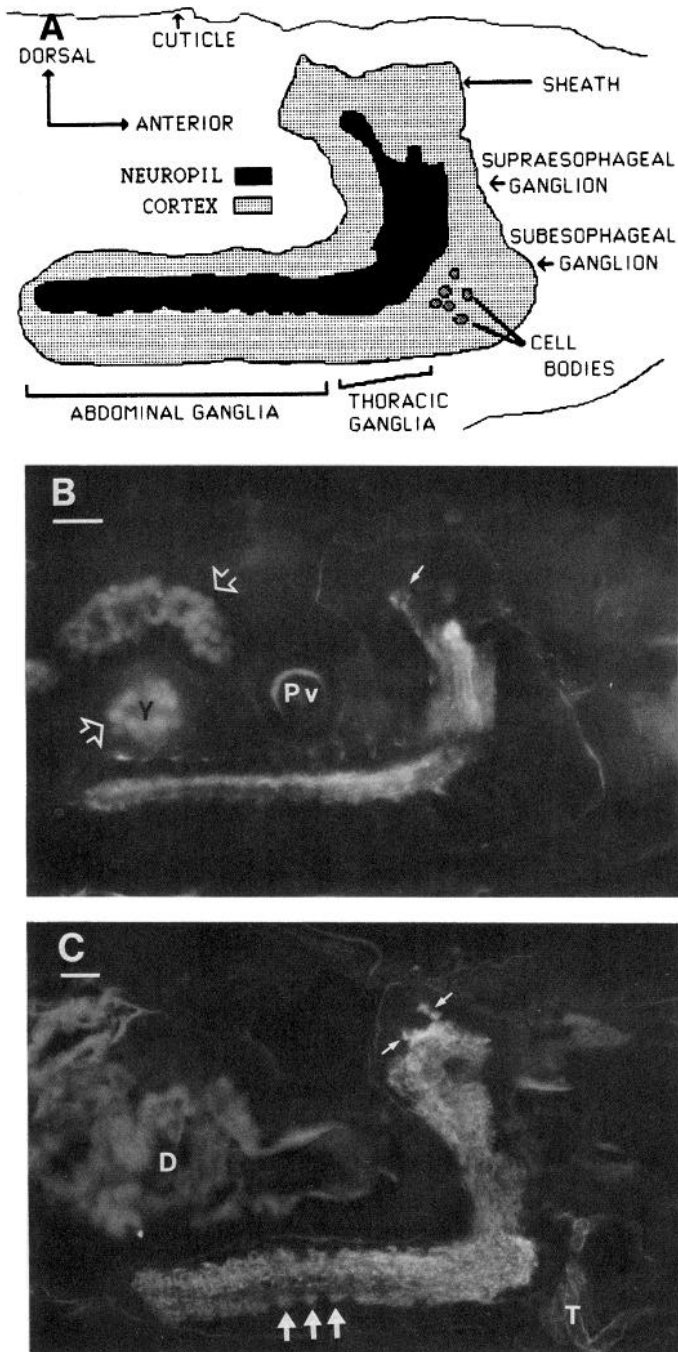
Figure 1. CAT immunoreactivity in sagittal sections of the embryonic and larval CNS. *A*, Schematic representation of the 16–18 hr embryonic nervous system. *B*, A 16–18 hr embryo: FITC-labeled secondary antibody specifically stains the developing neuropil region. *Solid arrow* points to what is probably the calyx of the corpora pedunculata (mushroom body). The proventriculus (*Pv*) and yolk (*Y, open arrows*) were stained red by the antiquenching compound PD (see Materials and Methods). *C*, Second instar larva: The neuropil staining region now occupies a greater proportion of the CNS volume, and the enlarged supraesophageal ganglion comprises most of the developing brain lobe. Uppermost staining region in the brain (*small arrows*) is the calyx. *Larger arrows* point to 3 contiguous abdominal neuromeres. The large diffuse mass posterior to the brain is the digestive system (*D*), which was stained red by PD. Trachea (*T*) also stained. Scale bar, 20 μm.

imals examined, all exhibited a similar staining pattern in the nervous system that was clearly greater in intensity than in other organs (Fig. 1, *A, B*). Immunoreactivity was primarily localized to the neuropil region, yet cell bodies could also be observed to stain dimly. Segmentation in the abdominal ganglia was obvious; 7 or more neuromeres could often be counted. Staining was also observed in the anterior region of the embryo where the antennal and maxillary ganglia are located (not shown). Staining of the more fully developed CNS ($n = 10$) in 18- to 20-hr-old embryos (ca. 2–4 hr before hatching) was considerably brighter, though qualitatively similar.

Larvae

The pattern of immunoreactivity in first instar larvae ($n = 5$) was very similar to that of late embryos. By the second larval instar ($n = 5$), the staining neuropil region comprised a much greater volume of the CNS (Fig. 1C). The brain lobes were readily discernible, and a structure at the top of the neuropil region, the calyx of the corpora pedunculata (mushroom body), stained brightly (see Bodenstein, 1950; Technau and Heisenberg, 1982). The CNS of third instar larvae ($n = 10$) was dissected out and fixed to optimize staining intensity (see Materials and Methods). Strong fluorescence of neuropil and some cell bodies resulted (Fig. 2, *A, B*). Immunoreactivity in the brain lobes was less extensive than in earlier larval instars because much of each hemisphere at this time is devoted to developing optic ganglia (White and Kankel, 1978), which are not immunoreactive with respect to CAT. Cell bodies and an axon are readily discernible in Figure 2B. A fiber tract, probably Bolwig's nerve, from the larval photosensitive organ (see Venkatesh et al., 1985), emanates from the lateral edge of the brain lobe in the region of the developing lamina and travels centrally, where it terminates in a diffuse, glowing mass. These fibers are likely candidates for cholinergic sensory afferents.

Pupae

Pupal nervous systems were examined 12, 36, 48, 60, 66, 72, 80, and 96 hr after the white prepupal stage. As with third instar larvae, the CNS was dissected out and fixed. Three brains from each stage were examined. At 12 hr, immunoreactivity was relatively bright and reminiscent of late third instar larvae. Clusters of brightly staining cell bodies existed in several regions, with the most prominent lying along the posterior midline of the brain. A prominently stained fiber tract projected from the developing distal optic lobe to the midbrain. By 36 hr, the general intensity of staining had noticeably decreased. Immunoreactivity was difficult to observe at 48 hr and disappeared almost entirely by 60 hr. By 66 hr, it had increased slightly; at this stage, only the ventral tubercles (Power, 1943) were stained well enough to be recognized. These structures are located in the central brain, in a region dorsal to the esophagus (see Fig. 4D). By 80 hr, faint staining delineated many of the adult structures. Again, the tubercles were the exception, being very bright. By 96 hr, about 12 hr before eclosion, the staining pattern appeared essentially as it did in adults but was still substantially dimmer. A comparison of an adult and a late pupal head, processed on the same slide, is shown in Figure 3.

Adults

CAT immunoreactivity in the adult brain was widespread and, as in earlier developmental stages, was localized primarily to
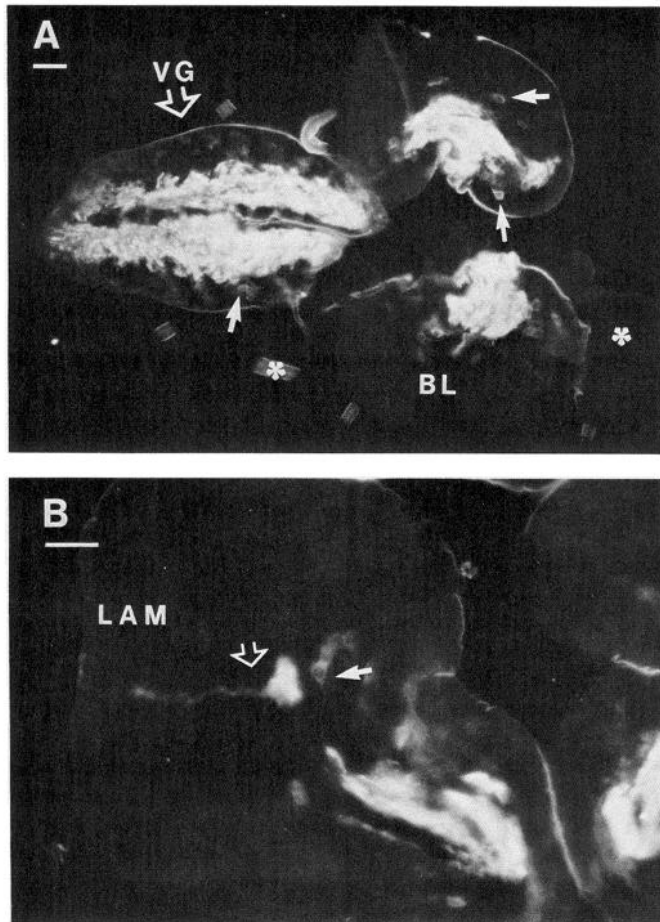
Figure 2. CAT immunoreactivity in late third instar larva. *A,* Horizontal section through brain lobes (*BL*) and ventral ganglia (*VG*) reveals many cell bodies (*arrows*) and brightly staining neuropil. Bits of trachea and part of an imaginal disk are visible outside the limits of the CNS (*asterisks*). Anterior is *right. B,* Frontal section through brain lobes showing a prominent nerve (see text) emanating from the periphery and its synaptic region (*open arrow*). *Solid arrow* points to a monopolar cell whose axon terminates in the subesophageal neuropil. Developing optic lamina (*Lam*) does not stain. Dorsal is to the *top.* Scale bar, 20 μm.

Figure 3. CAT immunoreactivity in a horizontal section of late pupa and adult. A 96 hr pupa, *left,* and a 2-d-old adult, *right,* possess morphologically similar optic lobes (*OL*), but the staining in the pupa is substantially less. Flies were mounted side by side on the same block. The pupa was removed from its case and prepared for fixation by peeling the outer membrane away from the mouthpart region and dissecting out the proboscis and ventral air sacs, thus exposing the brain directly to fixative. The adult was prepared in essentially the same fashion. Note that cuticle is highly autofluorescent. Scale bar, 100 μm.

neuropil areas. Figure 4*A* (specimen stained with Azure C) shows the various brain structures at a level just anterior to the esophagus. The dark cortical areas comprise a small percentage of the adult's brain volume. The neuropil structures visible as lightly stained areas in Figure 4*A* are readily discernible as CAT immunofluorescent regions in Figure 4*B.* Stained cell bodies can also be seen lateral and anterior to the antennal lobes. Many fiber tracts are apparent; a few of these, such as the antennal glomerular tract, stained brightly (Fig. 4, *C, D*). Another major tract, the peduncle of the mushroom body (Heisenberg et al., 1985), exhibited minimal staining (Fig. 4*C*). At the posterior apex of the peduncle is the calyx, an area dense with axon terminals from the antennal glomerular tract and Kenyon cell fibers; the latter continue anteriorly through the peduncle (Strausfeld, 1976; Heisenberg et al., 1985). The calyx was one of the most intensely immunoreactive regions of the adult brain. The central body and ventral tubercles of the central complex (Power, 1943) were well stained by the anti-CAT antibody. Small, brightly staining regions were noticeable at a number of locations, such as the lateral edge of the accessory protocerebral
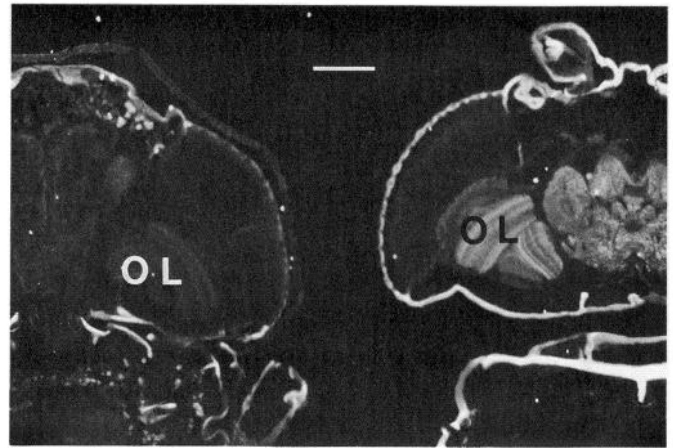
lobe (Fig. 4*C*) and the lateral border of the ventral protocerebral lobe adjacent to the lobula/medulla junction of the optic lobe complex (not shown).

The most obviously ordered structures in the *Drosophila* brain are the optic lobes (Fig. 5, *A, B*). Small cell bodies of laminar interneurons were clearly stained by anti-CAT in the distal lamina (Fig. 5*B*). Their fibers form the linear cartridges that converge at the first optic chiasm and comprise the bulk of the lamina along with photoreceptor terminals (e.g., Strausfeld, 1976). Just proximal to the laminar interneuron cell body layer there was an array of brightly staining spots (Fig. 5*B,* small arrows). Though their position is similar to the cell bodies located at the distal aspect of the cartridges seen in Figure 5*A* (small arrows), their inverted U-shaped symmetry (Fig. 5*B,* inset) is distinctly different from the circular form that cell bodies take. (Note the many adjacent laminar interneuron somata.) In addition, they are more immunoreactive than the laminar interneuron cell bodies. Proximal to these structures is the first optic chiasm. Fibers radiate from the chiasm and project to the medulla, where laminar interneurons termed type 1 and 2 (Strausfeld, 1976) synapse in a distal band; this stained strongly with anti-CAT antibody (Fig. 5*B,* black arrow). Numerous lesser staining bands were also delineated in the medulla; these were divided perpendicularly by columns of staining that represent the regular array of fibers from the lamina. A similar pattern was present in the lobula (see Fig. 7). Between the lobula and medulla, faintly staining fibers are visible as they decussate through the second optic chiasm.

In the ventral nervous system (Fig. 6), as in the brain, CAT immunoreactivity was primarily neuropil-specific. Few cell bodies were seen, but this might have been due to slow fixation since these ganglia, unlike the brain, were not directly exposed to fixative (see Materials and Methods). Numerous lightly staining nerves could be seen leaving the ganglia and projecting to the periphery. In midsagittal sections, remnants of the abdominal segmentation pattern, which is so obvious during embry-
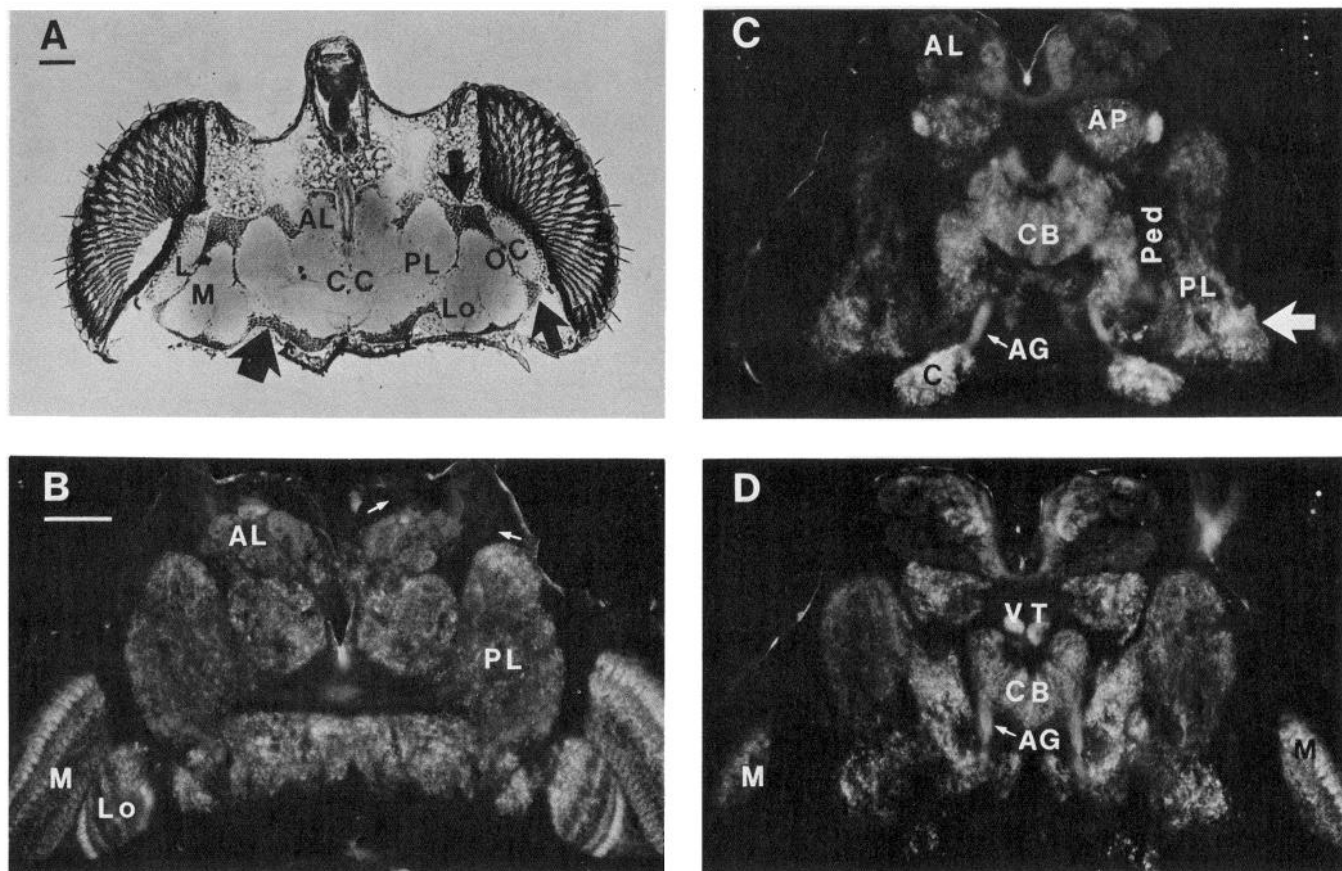
Figure 4. CAT immunoreactivity in the adult brain. *A,* Horizontal section through the head just dorsal to the esophagus. An unfixed fly was stained with Azure C. Cortex is designated by dark areas (*arrows*). Lighter staining regions bounded by the cortex are neuropil. *L,* lamina; *OC,* optic chiasm; *M,* medulla; *Lo,* lobula; *CC,* central commissure; *PL,* protocerebral lobe; *AL,* antennal lobe. *B,* CAT immunofluorescent staining of similar region to *A* but enlarged 2-fold to show more detail. Almost the entire neuropil stains at this plane of section, though certain regions such as the medulla and lobula have particularly immunoreactive layers. Some staining neuronal cell bodies are located laterally and anteriorly to the antennal lobes (*arrows*). *C,* Dorsal brain of adult. Prominent staining is visible in the calyx (*C*) of the corpora pedunculata, the antennal glomerular tract leading to it (*AG*), the lateral/posterior aspect of the protocerebral lobes (*arrow*), and the lateral border of the accessory protocerebral lobes (*AP*). The peduncles (*Ped*), fiber tracts that project anteriorly from the calyx to the AP, exhibit minimal immunoreactivity. *D,* Section 10 μm ventral to *C*. The AG dips below the central body (*CB*) in its course to the antennal lobe. The dorsal tips of the ventral tubercles (*VT*) are visible in the concave aspect of the central body. The dorsal rim of the medulla (*M*) can be seen to the extreme *left* and *right*. Anterior is to the *top*. Scale bars, 40 μm. *C* and *D* are same scale as *B*.

onic and larval development, were visible (not shown). This metameric organization consisted of minute, ventrally oriented protuberances. At the anterior end of the prothoracic ganglion, dorsal to the cervical connective and anterior to the cardia (an alimentary structure), is the stomatodaeal (stomatogastric) ganglion (Miller, 1950). Immunoreactivity was localized to a small area within its confines (not shown).

Areas other than the CNS were also immunoreactive. Neuronal cell bodies in the antenna and in the haltere stalk were faintly stained in some preparations. Considering that cell bodies generally do not stain very brightly, and that both these cuticle-covered organs were not directly exposed to fixative, the immunoreactivity was probably specific and not just "high background."

No immunoreactivity was seen at the base of bristles where mechanosensory somata are located (Burg and Wu, 1986). However, this negative result could have been an artifact resulting from the small size of such cell bodies, cuticular autofluorescence, and the fact that cell bodies, in general, do not stain intensely (see above).

Mutant immunoreactivity

The patterns of CAT immunoreactivity in the temperature-sensitive *Cha* mutants were first examined at 18°C, the permissive temperature (permissive and nonpermissive being defined on the basis of lethality, not enzyme activity). The results for the controls, *Cha+/Cha+* (wild-type, which carries 2 normal copies of the CAT gene) and *Cha+/Df-Cha* (only 1 normal copy), and the mutants, *Cha^{ts2}/Df-Cha* and *Cha^{ts1}/Df-Cha* (both of which carry only 1 copy of the CAT gene, which is mutant), are shown in Figure 7. The micrographs were taken from 2 adjacent sections that contained flies of all 4 genotypes that had been prepared identically and mounted in the same specimen block. Table 1 compares CAT activity (see Greenspan, 1980) to these levels of immunoreactivity. *Cha+/Cha+* (100% CAT activity), is noticeably more immunoreactive than *Cha+/Df-Cha* (50% CAT activity; $n = 10$ for each genotype). *Cha^{ts2}/Df-Cha*, the more severe mutant with regard to CAT activity, exhibited virtually no staining ($n = 5$). Immunoreactivity was essentially absent unless the time of the staining reaction was lengthened
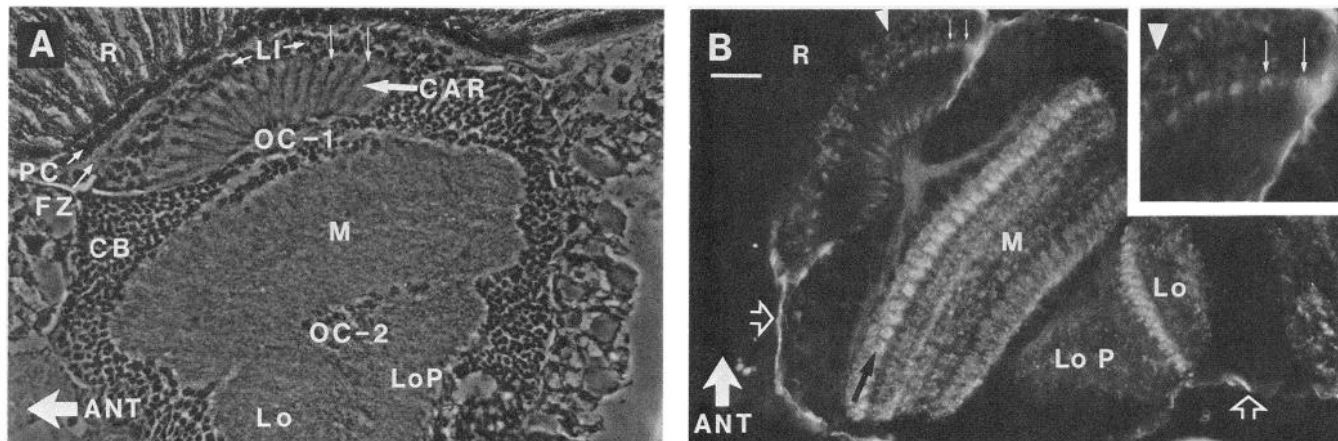
Figure 5. CAT immunoreactivity in the adult optic lobes. *A,* Horizontal section stained with Azure C. *R,* retina; *PC,* pigment cell layer; *FZ,* fenestrated zone; *CB,* neuronal cell bodies; *LI,* laminar interneuron cell body layer; *CAR,* optic cartridge; *OC-1,* first optic chiasm; *M,* medulla; *OC-2,* second optic chiasm; *Lo,* lobula; *LoP,* lobula plate. *Small arrows* point to cell bodies (see inset, described below). *B,* Similar section labeled with anti-CAT antibody. Note the absence of staining in retina (*R*). Cell bodies of laminar interneurons stain prominently (*triangle*). The fibers in both optic chiasmata can be seen. *Black arrow* is directed at medullary layer where laminar interneurons synapse. *Open arrows* point to membrane surrounding the CNS. *Inset,* a 2-fold enlargement of the right side of the lamina showing the inverted U-shaped structures described in text (*arrows*). Note that different orientation of lobula and lobula plate is due to a right (*A*) vs left (*B*) eye. Anterior, *ANT*. Scale bar, 20 μm.

to enhance the HRP reaction product; even then, staining was still very faint. However, $Cha^{ts1}/Df\text{-}Cha$ showed substantial immunoreactivity, more than $Cha^+/Df\text{-}Cha$ (n = 7 for each genotype), even though $Cha^{ts1}/Df\text{-}Cha$ has only a mutant copy of the CAT gene. Surprisingly, $Cha^{ts1}/Df\text{-}Cha$ stained as strongly as Cha^+/Cha^+ (n = 10 for each genotype). In other words, levels of CAT immunoreactivity with 1 copy of a mutant gene were essentially the same as with 2 copies of the wild-type gene. The above results were clearly demonstrated in all specimens regardless of whether the flies were mounted together or separately.

When flies were incubated at 30°C, sectioned, and stained, immunoreactivity decreased somewhat in both $Cha^{ts1}/Df\text{-}Cha$ and $Cha^{ts2}/Df\text{-}Cha$; in the latter case, this was apparent only when the time of the staining reaction was lengthened to enhance the HRP reaction product. In $Cha^{ts1}/Df\text{-}Cha$, the laminar interneuron and optic chiasm staining disappeared between 24 and 48 hr. There was also a general, though less dramatic decrease in neuropil immunoreactivity. However, even after 72 hr of incubation at 30°C (resulting in a decrease to about 2% of normal CAT activity; Greenspan, 1980), some staining was still apparent. In $Cha^{ts2}/Df\text{-}Cha$, staining was very low to begin with and was not visible after 36–48 hr of incubation at 30°C (which results in a decrease to about 2% of normal CAT activity; Greenspan, 1980). This level of staining (or its absence) defined the background. This result also served as a control for nonspecific

staining that might have been detected by this antibody; apparently, there was none.

Preliminary studies of mutants that were unconditionally CAT-negative with respect to enzyme activity (Greenspan, 1980) were also made. Since these mutants possessed no detectable CAT activity, lethality occurred late in the embryonic stage. Of the few late embryos examined, the CAT-negative sections displayed no staining in the nervous system compared with the faint staining in the control sections (not shown).

Discussion

CAT immunoreactivity in wild-type Drosophila

Immunoreactive staining of choline acetyltransferase molecules with monoclonal antibodies was first apparent in 16–18 hr em-

Table 1. CAT activity versus immunoreactivity in *Cha^{ts}* mutants and control flies raised at permissive temperature

	$\dfrac{Cha^+}{Cha^+}$	$\dfrac{Cha^+}{Df\text{-}Cha}$	$\dfrac{Cha^{ts1}}{Df\text{-}Cha}$	$\dfrac{Cha^{ts2}}{Df\text{-}Cha}$
Enzyme activity[a]	100	54	34	8
Immunoreactivity	++	+	++	−

Plus and minus symbols represent our visual assessment of immunoreactive intensity.

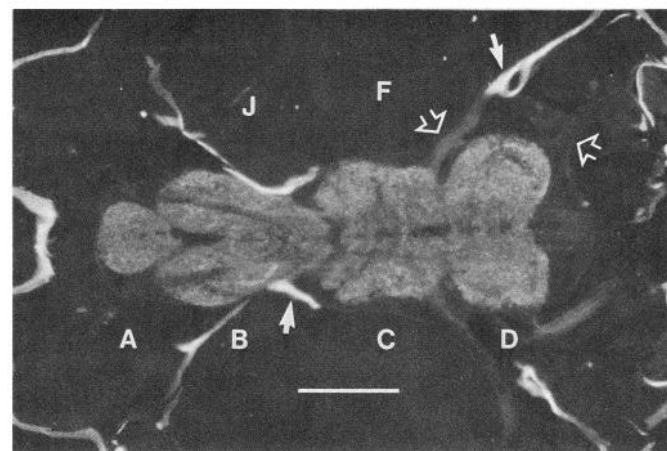[a] Percentage of wild-type CAT activity data from Greenspan (1980).

Figure 6. CAT immunoreactivity in the ventral nervous system of adult flies. The 3 thoracic ganglia and the abdominal ganglion are evident in this horizontal section. A number of nerves can be seen leaving the ganglia (*open arrows*). Very bright staining regions (*closed arrows*) are autofluorescing cuticle. The flight (*F*) and jump (*J*) muscles surround the bulk of the ganglia. *A,* Abdominal ganglion; *B,* metathoracic ganglion; *C,* mesothoracic ganglion; *D,* prothoracic ganglion. Anterior is *right.* Scale bar, 100 μm.
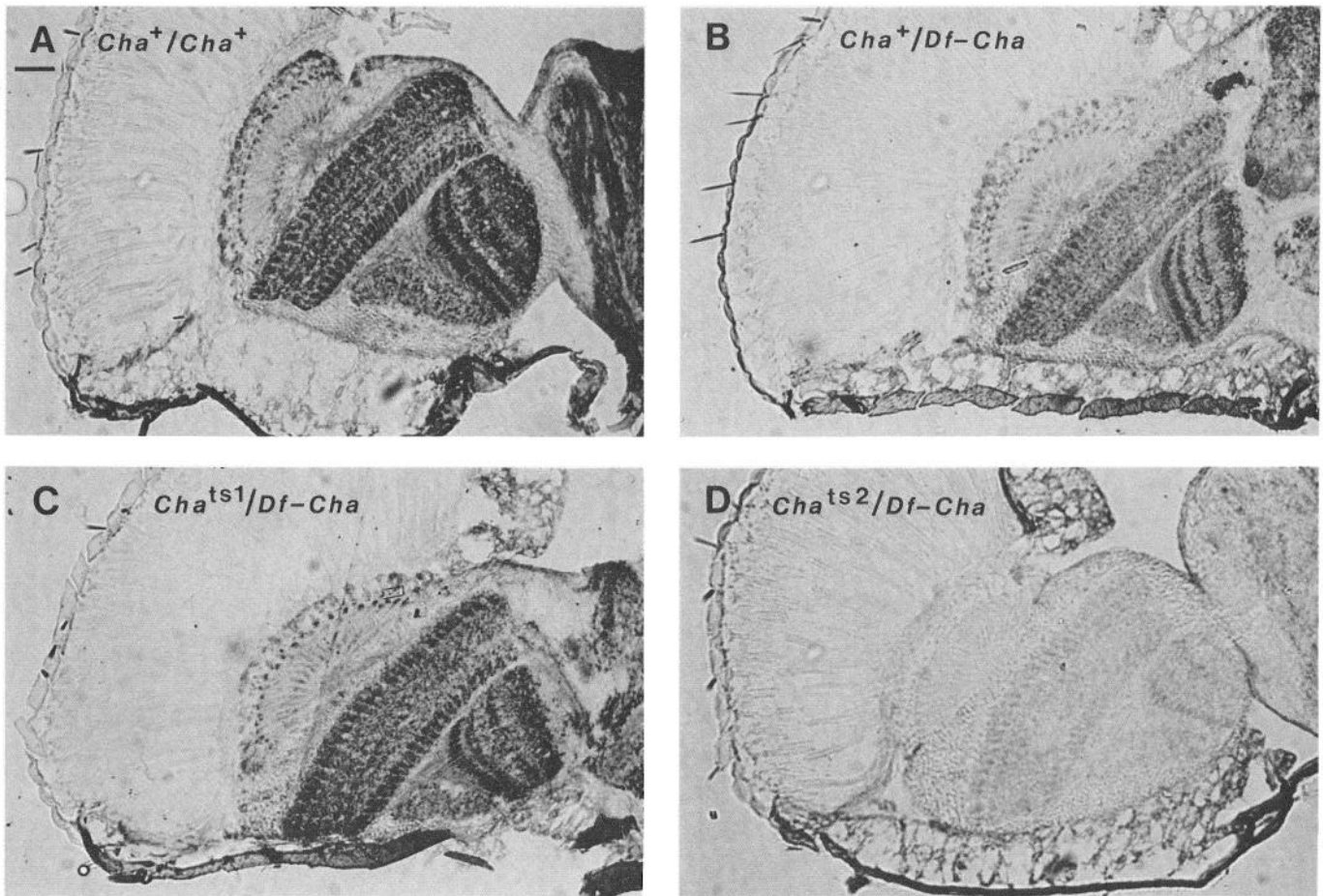
Figure 7. CAT immunoreactivity in *Cha* mutants raised at permissive temperature. Four fly heads were mounted together and processed identically for the HRP reaction product. Photographs were taken from 2 adjacent sections. Exposure times and photographic procedures were identical. Anterior is *right*. Scale bar, 20 μm.

bryos. This was anticipated from earlier studies that involved biochemical assays of enzyme activity; a slight increase in CAT activity above the background level was noted at 13 hr, followed by a rather rapid increase that continued until the end of embryogenesis (Dewhurst and Seecof, 1975). It is known that neuronal outgrowth and growth cone target choices occur between hours 10 and 13, whereas synaptogenesis commences shortly afterwards (Goodman et al., 1984). Synthesis of CAT occurs in concert with these developments.

The relatively constant intensity of staining throughout most of larval development is consistent with previous biochemical studies (Dewhurst et al., 1970). That CAT staining is localized primarily to neuron terminals is expected because the enzyme is found in synaptic endings, where it synthesizes ACh from acetyl-CoA and choline (Cooper et al., 1982). Presumably, in cells where synthesis of CAT is high, the somata would also be immunoreactive.

In sections from third instar larvae, fibers that are likely to have been sensory afferents from Bolwig's nerve were stained, as was a structure that appeared to be the area of synaptic terminals for these neurons. The possibility that these putative sensory afferents are cholinergic is consistent with findings on sensory afferents from *Periplaneta* (Satelle et al., 1980) and *Manduca* (Sanes et al., 1977).

In pupae, there was a gradual decline in immunoreactivity

that reached a nadir between 48–60 hr, at which time the staining was just above background levels. After this time, there was a continual increase in staining in the developing pupa. Coincident with these changes, CAT activity in pupae has been shown to decrease from the white prepupal period to its lowest level, between hours 48 and 72, followed by a slow increase until the last day before emergence; at that stage, activity levels rapidly reach their maximum (Dewhurst et al., 1970). Low CAT activity and staining appear to coincide with the "breakdown" of parts of the larval nervous system and the remodeling of ganglia involved in building the adult CNS form (White and Kankel, 1978; Technau and Heisenberg, 1982; White et al., 1983).

Immunoreactivity in the adult was extensive, with many neuropil structures being well delineated by their respective staining intensity. Discrete areas that are not revealed by conventional stains (e.g., toluidine), such as the lateral borders of the accessory protocerebral lobe (Fig. 4C), were found to be very immunoreactive. Anti-CAT antibodies could prove valuable in this regard, since most stains are not specific for nervous tissue. They do not exhibit differential staining ability, i.e., the nervous system appears monochromatic, and structural distinctions within it are difficult to ascertain (see Fig. 4A). Thus, the relative abundance of CAT immunoreactivity in different structures and tracts within the adult CNS serves as a novel histological marker. For example, the non-staining peduncles of the mushroom bodies

are well delineated in adult brains stained with this antibody (Fig. 4C).

In the adult lamina, a layer of inverted U-shaped immuno-reactive structures was found just below the laminar interneuron cell body layer (Fig. 5B, inset). Though they share a similar position with an unidentified array of cell bodies in that region (Fig. 5A), it is doubtful that they are neuronal somata. The reasons for this are that they stained substantially more intensely than any cell bodies in the brain and that they did not possess a circular symmetry as do cell bodies. Also, the arms of the "U" seem to be contiguous with faintly staining fibers. It is probable that they are synaptic terminals from intrinsic or centripetally projecting neurons (Strausfeld, 1976).

The 2 areas where cell bodies are most prominent are the laminar interneuron layer and areas adjacent to the antennal lobes. The laminar interneurons synapse in the very densely staining regions of the medulla (Strausfeld, 1976). Though it is not known exactly what targets are innervated by the neurons adjacent to the antennal lobes, their fibers might travel in the antennal glomerular tract, which terminates in the calyx of the mushroom bodies and the dorsal lateral protocerebral lobe (Strausfeld, 1976; Heisenberg et al., 1985); both of these structures stained intensely with anti-CAT antibody (Fig. 4C). There were also 2 areas in the PNS where stained cell bodies were recognized. These were located at the base of the antenna and in the haltere stalk; in the latter case, they were probably the cell bodies of sensory neurons from the campaniform sensilla that cover the stalk. Their faint staining may have been due, in part, to poor access to fixative (see Materials and Methods).

Ikeda et al. (1984) have published a preliminary report on anti-CAT staining in the optic lobe and various neuropil regions of adult *D. melanogaster* brain using a different MAb against *Drosophila* CAT, termed 1G4 (Crawford et al., 1982). The staining pattern (Salvaterra et al., 1985) for the 1 section reported (through the adult brain) appeared to be very similar to the results reported here (e.g., Fig. 7A). A concomitant determination of α-BTX binding distribution was made and said to closely correspond with CAT staining in specific bands of the medulla (Ikeda et al., 1984). However, the relation between ACh receptors and α-BTX binding sites is unclear, and the colocalization of α-BTX binding sites and CAT may simply be fortuitous; i.e., the former may not mark cholinergic portions of the CNS in *Drosophila* (Wu et al., 1983; Clarke et al., 1985; Smith et al., 1985).

Results from a study of choline uptake in *Drosophila* brain (Buchner and Rodrigues, 1984) do not correspond to the results reported here. Autoradiographs of tritiated choline distribution showed labeling in the antennal lobes, the antennal mechanosensory area, and the ventral medial subesophageal ganglion. No grains were observed in the optic lobes or in the supraesophageal ganglion. The authors mentioned that their results were difficult to reconcile with previous genetic, pharmacological, and physiological evidence for cholinergic activity in the optic lobes (Dudai, 1980; Greenspan, 1980; Greenspan et al., 1980). We concur, in the sense that our descriptions of CAT immunoreactivity are readily reconcilable with the experimental results just cited.

Staining in Cha^{ts} mutants

The difference in degree of immunoreactivity between *Cha$^+$/ Cha$^+$* and *Cha$^+$/Df-Cha* was not unexpected because *Cha$^+$/Df-*

Cha carries only 1 copy of the gene instead of 2, and probably produces the CAT protein at 50% of the wild-type level, as is suggested by the enzyme activity (Greenspan, 1980). However, the density of staining in the *Cha^{ts}* mutants was more difficult to predict. In these flies, the concentration of CAT molecules could be reduced, or these mutations could lead to an altered protein structure that would account for lowered enzyme activity. A decrease in the concentration of this enzyme would be expected to cause less staining, whereas a change in structure could lead to more, less, or no change in the staining.

At permissive temperature, immunoreactivity in *Cha^{ts1}/Df-Cha* was as high as in wild-type. Since 1 copy of the gene is deleted, the staining intensity might have been expected to be no more than half normal; i.e., corresponding to the *Cha$^+$/Df-Cha* control, in which reduced staining was indeed noticeable (Fig. 7B). The *Cha^{ts1}* genotype involves not only a half-normal dosage of this gene but a mutated one as well. A change in the concentration of CAT molecules is insufficient to account for both the reduction in enzyme activity and the increase in immunoreactivity at permissive temperature for *Cha^{ts1}/Df-Cha*. We suggest that this mutation has led to an alteration in the enzyme's primary structure. This hypothesis has been presented previously by Gorczyca and Hall (1984) and Salvaterra and McCaman (1985), based on various physiological and biochemical analyses, respectively, of the conditional *Cha^{ts}* mutants.

In the other mutant of this type, *Cha^{ts2}/Df-Cha*, CAT immunoreactivity is essentially eliminated (Fig. 7D). This served as a control for nonspecific staining elicited by the antibody. Since there was none, we believe that MAb 1C8 exclusively binds to CAT in wild-type and *Cha^{ts1}* flies. The absence of staining can be explained by either a decrease in the number of CAT molecules and/or a qualitative change in the structure of the enzyme.

At nonpermissive temperature, CAT staining decreased slightly in both *Cha^{ts}* mutants. This result is at least qualitatively similar to that of Ikeda et al. (1984), who used a different anti-CAT MAb. They reported, in contrast to our results, that immunoreactivity of both *Cha^{ts}* mutants at permissive temperature was lower than wild-type and decreased substantially and relatively quickly upon incubation at 30°C. That MAb 1G4 (Ikeda et al., 1984) vs 1C8 (this report) lead to different staining intensities from experiments on these conditional mutants buttresses the suggestion that these 2 monoclonal antibodies recognize different epitopes (Slemmon et al., 1982). In addition, we now suggest that the antigenic determinant recognized by 1G4 seems to be more thermolabile than the determinant for 1C8.

Since *Cha^{ts2}/Df-Cha* exhibits almost no immunoreactivity, it would be a very useful genotype for mosaic studies of cholinergic function. That is, flies could be produced which are part *Cha$^+$* and part *Cha^{ts2}*. After an appropriate temperature-treatment (see Greenspan, 1980), various behavioral and physiological abnormalities could be probed [see Greenspan et al.'s studies of analogous AChE mosaics (1980)]. The aim would be to relate various functional impairments to spatially and temporally known turn-offs of ACh synthesis. Thus, after sectioning and histochemistry of these *Cha$^+$//Cha^{ts2}* mosaics, the CAT-negative tissue could be readily identified, given the results we now report.

In summary, CAT immunoreactivity was found to be extensive in the developing and adult nervous system of *D. melanogaster*, a result that attests to a major role for ACh in the insect CNS. Mutant analysis confirmed the specificity of the antibody to the enzyme molecule and provided strong support

for the suggestion that at least 1 mutant, Cha^ts1, possesses a structurally altered CAT molecule.

Note added in proof: A similar study, though restricted to wild-type adult brain, was recently published (Buchner et al., 1986).

References

Bodenstein, D. (1950) The postembryonic development of *Drosophila*. In *Biology of Drosophila*, M. Demerec, ed., pp. 275–367, Hafner/Wiley, New York.

Buchner, E., and V. Rodrigues (1984) Autoradiographic localization of [³H]choline uptake in the brain of *Drosophila melanogaster*. Neurosci. Lett. *42:* 25–31.

Buchner, E., S. Buchner, G. Crawford, W. T. Mason, P. M. Salvaterra, and D. B. Sattelle (1986) Choline acetyltransferase-like immunoreactivity in the brain of *Drosophila melanogaster*. Cell Tissue Res. *246:* 57–62.

Burg, M., and C.-F. Wu (1986) Differentiation and central projections of peripheral sensory cells with action-potential block in *Drosophila* mosaics. J. Neurosci. *6:* 2968–2976.

Callec, J. J. (1976) Synaptic transmission in the central nervous system of insects. In *Insect Neurobiology*, Vol. 35, J. E. Treherne, ed., pp. 119–186, North-Holland, Amsterdam.

Clarke, P. B., R. Schwartz, S. Paul, C. Pert, and A. Pert (1985) Nicotinic binding in rat brain: Autoradiographic comparison of [³H] acetylcholine, [³H] nicotine, and [¹²⁵I]-alpha-bungarotoxin. J. Neurosci. *5:* 1307–1315.

Cooper, J. R., F. E. Bloom, and R. H. Roth (1982) Acetylcholine. In *The Biochemical Basis of Neuropharmacology*, 4th ed., pp. 77–108, Oxford U. P., New York.

Crawford, G., J. R. Slemmon, and P. M. Salvaterra (1982) Monoclonal antibodies selective for *Drosophila melanogaster* choline acetyltransferase. J. Biol. Chem. *7:* 3853–3856.

Dewhurst, S. A., and R. L. Seecof (1975) Development of acetylcholine metabolizing enzymes in *Drosophila* embryos and in cultures of embryonic *Drosophila* cells. Comp. Biochem. Physiol. *50C:* 53–58.

Dewhurst, S. A., R. E. McCaman, and W. D. Kaplan (1970) The time course of development of acetylcholine and choline acetyltransferase in *Drosophila melanogaster*. Biochem. Genet. *4:* 499–508.

Dudai, Y. (1980) Cholinergic receptors of *Drosophila*. In *Receptors for Neurotransmitter, Hormones, and Pheromones in Insects*, D. B. Sattelle, L. M. Hall, and J. G. Hildebrand, eds., pp. 93–110, Elsevier, Amsterdam.

Eckenstein, F. (1985) Antibodies to acetylcholine at last. Nature *318:* 236.

Florey, E. (1963) Acetylcholine in the invertebrate nervous system. Can. J. Biochem. Physiol. *41:* 2619–2626.

Gerschenfeld, H. M. (1973) Chemical transmission in invertebrate central nervous systems and neuromuscular junctions. Physiol. Rev. *53:* 1–119.

Goodman, C. S., M. J. Bastiani, M. J. Doe, S. du Lac, S. L. Helfand, J. Y. Kuwada, and J. B. Thomas (1984) Cell recognition during neuronal development. Science *225:* 1271–1279.

Gorczyca, M. G., and J. C. Hall (1984) Identification of a cholinergic synapse in the giant fiber pathway of *Drosophila* using conditional mutations of acetylcholine synthesis. J. Neurogenet. *1:* 289–313.

Gorczyca, M. G., and J. C. Hall (1985) Effects of neurochemical and neuroanatomical mutants on the landing response and flight muscle activity of *Drosophila melanogaster*. Soc. Neurosci. Abstr. *15:* 512.

Greenspan, R. J. (1980) Mutations of choline acetyltransferase and associated neural defects in *Drosophila melanogaster*. J. Comp. Physiol. *137:* 83–92.

Greenspan, R. J., J. A. Finn, and J. C. Hall (1980) Acetylcholinesterase mutants in *Drosophila* and their effects on the structure and function of the nervous system. J. Comp. Neurol. *189:* 741–774.

Harrow, I. D., J. A. David, and D. B. Satelle (1982) Acetylcholine receptors of identified insect neurons. In *Neuropharmacology of Insects*, D. Evered, M. O'Connor, and J. Whelan, eds., pp. 12–31, Ciba Foundation, Pitman, London.

Heisenberg, M., A. Borst, S. Wagner, and D. Byers (1985) *Drosophila* mushroom body mutants are deficient in olfactory learning. J. Neurogenet. *2:* 1–30.

Ikeda, K., P. M. Salvaterra, G. Crawford, and D. A. Matthews (1984)

Immunocytochemical study of choline acetyltransferase in wild type and mutant *Drosophila melanogaster*. Soc. Neurosci. Abstr. *10:* 442.

Itoh, N., J. R. Slemmon, D. H. Hawke, R. Williamson, E. Morita, K. Itakura, E. Roberts, J. E. Shively, G. D. Crawford, and P. M. Salvaterra (1986) Cloning *Drosophila* choline acetyltransferase cDNA. Proc. Natl. Acad. Sci. USA *83:* 4081–4085.

Klemm, N. (1976) Histochemistry of putative transmitter substances in the brain. Prog. Neurobiol. *7:* 99–169.

Miller, A. (1950) The internal anatomy and histology of the imago of *Drosophila melanogaster*. In *Biology of Drosophila*, M. Demerec, ed., pp. 420–534, Wiley, New York.

Mitchison, T. J., and J. Sedat (1983) Localization of antigenic determinants in whole *Drosophila* embryos. Dev. Biol. *99:* 261–264.

Platt, J. L., and A. F. Michael (1983) Retardation of fading and enhancement of intensity of immunofluorescence by *p*-phenylenediamine. J. Histochem. Cytochem. *31:* 840–842.

Power, M. E. (1943) The brain of *Drosophila melanogaster*. J. Morphol. *72:* 517–559.

Rudloff, E., F. Himenez, and F. Bartels (1980) Purification and properties of the nicotinic acetylcholine receptor of *Drosophila melanogaster*. In *Receptors for Neurotransmitter, Hormones, and Pheromones in Insects*, D. B. Satelle, L. M. Hall, and J. G. Hildebrand, eds., pp. 85–92. Elsevier, Amsterdam.

Salvaterra, P. M., and R. E. McCaman (1985) Choline acetyltransferase and acetylcholine levels in *Drosophila melanogaster*: A study using two temperature-sensitive mutations. J. Neurosci. *5:* 903–910.

Salvaterra, P. M., G. D. Crawford, G. D. Klotz, and K. Ikeda (1985) Production and use of monoclonal antibodies to biochemically defined insect neuronal antigens. In *Neurochemical Techniques in Insect Research*, H. Breer and T. A. Miller, eds., pp. 223–242, Springer-Verlag, New York.

Sanes, J. R., and J. G. Hildebrand (1976) Acetylcholine and its metabolic enzymes in developing antennae of the moth, *Manduca sexta*. Dev. Biol. *52:* 105–120.

Sanes, J. R., D. J. Prescott, and J. G. Hildebrand (1977) Cholinergic neurochemical development of normal and deafferented antennal lobes during metamorphosis of the moth, *Manduca sexta*. Brain Res. *119:* 389–402.

Satelle, D. B., J. A. David, I. D. Harrow, and B. Hue (1980) Actions of alpha-bungarotoxin on identified insect central neurons. In *Receptors for Neurotransmitter, Hormones, and Pheromones in Insects*, D. B. Satelle, L. M. Hall, and J. G. Hildebrand, eds., pp. 125–139, Elsevier, Amsterdam.

Schmidt-Nielson, B. K., J. I. Gepner, N. N. H. Teng, and L. M. Hall. (1977) Characterization of an alpha-bungarotoxin binding component from *Drosophila melanogaster*. J. Neurochem. *29:* 1013–1031.

Slemmon, J. R., P. M. Salvaterra, G. D. Crawford, and E. Roberts (1982) Purification of choline acetyltransferase from *Drosophila melanogaster*. J. Biol. Chem. *7:* 3847–3852.

Smith, M. A., J. Stollberg, J. M. Lindstrom, and D. K. Berg (1985) Characterization of a component in chick ciliary ganglia that cross-reacts with monoclonal antibodies to muscle and electric organ acetylcholine receptor. J. Neurosci. *5:* 2726–2731.

Strausfeld, N. J. (1976) *Atlas of an Insect Brain*, Springer-Verlag, New York.

Technau, G., and M. Heisenberg (1982) Neural reorganization during metamorphosis of the corpora pedunculata in *Drosophila melanogaster*. Nature *295:* 405–407.

Treherne, J. E. (1966) Acetylcholine. In *The Neurochemistry of Arthropods*, pp. 93–109, Cambridge U. P., Cambridge, U.K.

Vallés, A. M., and K. White (1986) Development of serotonin-containing neurons in *Drosophila* mutants unable to synthesize serotonin. J. Neurosci. *6:* 1482–1491.

Venkatesh, T. R., S. L. Zipursky, and S. Benzer (1985) Molecular analysis of the development of the compound eye in *Drosophila*. Trends Neurosci. *8:* 251–257.

White, K., and D. R. Kankel (1978) Patterns of cell division and cell movement in the formation of the imaginal nervous system in *Drosophila melanogaster*. Dev. Biol. *65:* 296–321.

White, K., A. Pereira, and L. E. Cannon (1983) Modulation of a neural antigen during metamorphosis in *Drosophila melanogaster*. Dev. Biol. *98:* 239–244.

Wu, C.-F., S. H. Young, and M. A. Tanouye (1983) Single channel recording of alpha-bungarotoxin resistant acetylcholine channels in dissociated CNS neurons of *Drosophila*. Soc. Neurosci. Abstr. *9:* 507.